

Development of a Platelet Lysate–Based Printable, Transparent Biomaterial With Regenerative Potential for Epithelial Corneal Injuries

Hannah Frazer¹, Jingjing You¹, Zhi Chen², Sepidar Sayyar^{2,3}, Xiao Liu², Adam Taylor², Chris Hodge^{1,2,4}, Gordon Wallace^{2,3}, and Gerard Sutton^{1,2,4}

¹ Save Sight Institute, Sydney Medical School, University of Sydney, Sydney, Australia

² ARC Centre of Excellence for Electromaterials Science, Intelligent Polymer Research Institute, AIIM, Innovation Campus, University of Wollongong, Wollongong, Australia

³ Australian National Fabrication Facility—Materials Node, Innovation Campus, University of Wollongong, Wollongong, Australia

⁴ NSW Tissue Bank, Sydney, Australia

Correspondence: Jingjing You, Save Sight Institute, Sydney Medical School, University of Sydney; Sydney, Australia. e-mail: jing.you@sydney.edu.au

Received: August 21, 2020

Accepted: November 17, 2020

Published: December 23, 2020

Keywords: human platelet lysate; bioink; corneal wound healing; fibrin

Citation: Frazer H, You J, Chen Z, Sayyar S, Liu X, Taylor A, Hodge C, Wallace G, Sutton G. Development of a platelet lysate–based printable, transparent biomaterial with regenerative potential for epithelial corneal injuries. *Trans Vis Sci Tech.* 2020;9(13):40. <https://doi.org/10.1167/tvst.9.13.40>

Purpose: To develop a human platelet lysate (hPL)–based bioink that is transparent and also encompasses the regenerative properties of hPL to facilitate wound healing.

Methods: The effect of different batches of hPL and fetal bovine serum (FBS) on corneal epithelial cell growth and scratch assay was first examined using Incucyte Zoom. Various combinations of human fibrinogen (concentration range from 0.2 to 5 mg/mL) and thrombin (concentration from 1 to 10 U/mL) were combined with hPL to generate nine types of potential bioink. Rheology, transparency, and cell compatibility of bioinks were assessed and compared. The final selected bioink was used in an ex vivo corneal model to examine its ability in re-epithelization.

Results: No significant difference was detected in cell proliferation and wound healing tests between different hPL batches at the same concentration. Scratch assay data showed that hPL had significantly higher effect on wound healing than FBS. Comparing across the nine bioinks, bioink 5 consisting of 10% hPL, 2 mg/mL fibrinogen, and 5 U/mL thrombin demonstrated all required mechanical and cellular properties and was able to regenerate the full-thickness epithelium ex vivo.

Conclusions: The results showed that a transparent and adhesive bioink can be generated by combining hPL, fibrinogen, and thrombin together. The bioink can be directly applied to a human cornea to promote corneal re-epithelization with huge potential applications in corneal injuries.

Translational Relevance: The developed transparent hPL-based ink with its adhesive and healing ability showed that it could be used as a new treatment option for corneal injuries.

Introduction

Corneal disease is the fifth leading cause of blindness globally, and a high percentage of cases with significant visual impairment are found in the developing world.^{1,2} The incidence of corneal-related visual loss because of infection and trauma is approximately 20 times greater in African and Asian countries compared to developed nations.³ The impact of corneal

injuries in all countries, however, remains significant. Corneal injuries such as foreign bodies and abrasions are the leading ophthalmic presentation to emergency in Australian hospitals. Direct and indirect costs related to these presentations was estimated at greater than AU\$155 million per year, indicating a significant financial burden.⁴

In mild cases of corneal trauma, the cornea is often able to regenerate via normal wound-healing pathways.⁵ This process, however, can take many days

and, because of the dense neural innervation of the cornea, is associated with significant pain. In some cases, the cornea's normal wound-healing mechanism may be insufficient.⁶ This leads to the formation of nonhealing defects, which can result in corneal melting,⁷ corneal neovascularization,⁸ loss of transparency, infection,² scarring, and diminished vision to the point of blindness.² In significant disease, corneal transplantation requiring donor tissue often represents the only visual rehabilitative option available to patients. This is problematic because only one in 70 patients worldwide has access to donor tissue.⁹ Prevention is therefore critical in reducing the burden of corneal blindness in the world.²

The goals of therapeutic treatment for corneal trauma are to restore the corneal surface, minimize damaging sequelae, and improve patient comfort. Recently, blood-derived treatments including peripheral blood serum, platelet lysate, umbilical cord blood serum, platelet-rich plasma (PRP), and plasma rich in growth factors have become popular in the treatment of ocular surface wounds.¹⁰ These products have potential advantages over current therapeutic options because they not only lubricate the ocular surface acting as a tear substitute, but also provide a source of a diverse range of growth factors and cytokines that facilitate wound healing.¹¹ All platelet-relevant products are derived from the base product, PRP, which can be prepared by separating the platelet components from whole blood with various centrifugation processes^{12,13} or through the use of an apheresis machine.¹⁴ These platelet-derived products are prepared either in the form of eye drops in which PRP or human platelet lysates (hPL) was used in its liquid form or as a bio-scaffold also called platelet clot/gel by exposing PRP or hPL to thrombin or calcium chloride to stimulate fibrin formation.¹⁵ The difference between hPL and PRP is that hPL refers to lysed PRP.¹⁵ A common method to lyse PRP is through freeze/thaw, which leads to platelet degranulation.¹⁵ The platelet clot/gel can be used as a dressing to aid in homeostasis restoration, tissue reparation, and regeneration.¹⁶ It has also been used in conjunction with both autologous fibrin membrane¹⁷ and bovine pericardium membrane¹⁸ to treat ocular perforations in more significant cases. It has been shown that platelet gel formation is part of the natural healing response that further enhances the delivery of platelet-derived growth factors.¹⁹ The potential benefits of platelet gel are offset by a lack of transparency that may impede visual rehabilitation, and, in comparison to fibrin gels, poor mechanical strength requires an additional membrane to hold it in place.^{17,18}

With the advent of 3D bio-printing, bioinks have been used to generate cell-laden tissues for rehabilitative purposes including for use on the human cornea.^{20,21} The printing process can be customized to the wound area and depth, thus having less geometrical limits and requiring less potential application time compared to standard molds.²² An emerging trend for the use of bioink in medical fields is in situ printing directly onto the injured site rather than bioprinting tissue that may then require additional application or suturing to the wounded area.²³ With respect to corneal injury and surface disease, developing a suitable bioink with the potential of in-situ application to the wounded cornea could have significant benefits, including reduced need for specialist application, immediate facilitation of the wound healing process, and improved patient comfort. By optimizing recovery in the acute injury stage, downstream treatments such as corneal transplantation may be avoided. This could be particularly advantageous in the developing world where access to specialist services and surgical options remains severely limited.

Development of bioinks in the field of corneal diseases is relatively recent, and their use currently are primarily around printing a bioengineered cornea ex vivo.^{20,21,24} The compositions of these bioinks are diverse. Isaacson et al.²⁰ and Kilic Bektas and Hasirci²⁴ both use non-human origin and modified proteins such as sodium alginate and methacrylated type I collagen and methacrylated gelatin²⁴ for extrusion printing a corneal stroma substrate. Sorkio et al.²¹ design two bioinks: one for epithelium and one for stroma. They use laser printing to construct a two-layered cornea structure with the two types of bioinks in which human recombinant laminin, hyaluronic acid sodium salt, human collagen I, blood plasma, and thrombin are used.²¹ Kim et al.²⁵ use decellularized cornea as the base of bioink for printing corneal-like structure. All studies endorse the importance of transparency. Kim et al.²⁵ and Kilic Bektas²⁴ show that their bioink has over 75% and 80% light transmittance, respectively, whereas Isaacson et al.²⁰ demonstrate the transparency by visual observation. However, the bioink developed by Sorkio et al.²¹ requires a nontransparent substance, Matrigel supportive sheets, to avoid shrinkage of the printed structure.

The key features for a successful bioink include high cell compatibility and proportionate mechanical properties. For the most commonly used extrusion-based 3D printers, two key physical properties for an ink are shear-thinning, whereby viscosity decreases under the shear encountered during printing, and the ability to undergo a phase transition such that the desired structural form is retained after

printing.²⁶ For use in corneal injuries, bioink transparency is an additional further consideration. In this study, we examined various hPL-based bioink formulations through cell-based and physical tests with the final goal of generating a suitable bioink capable of treating corneal injuries.

Materials and Methods

The Effect of hPL on Human Corneal Epithelial Cell Growth

A human SV40-adenovirus vector transformed corneal epithelial cell line (HCE-T; Riken Cell Bank, Ibaraki, Japan) was used. Cells were thawed, cultured, and maintained using hPL and fetal bovine serum (FBS), with FBS serving as a control. The control cells were cultured in FBS growth medium using the standard HCE-T growth medium consisting of 5% FBS, 10 ng/mL human epidermal growth factor (EGF),

5 µg/mL insulin, 50 µg/mL penicillin and streptomycin (p/s), and 2 mM glutamine (all reagents from Life Technologies, Carlsbad, CA, USA).

The hPL was obtained from the Australian Red Cross Blood Bank using expired buffy coat–derived platelet concentrates. The expired platelet concentrates were activated by freezing in –80°C and then thawing at 37°C. Three batches (batch CCP4, CCA4, and CCP5) derived from different pooled donors were used and examined. Among these three batches, CCP4 and CCP5 were from pooled platelets collected from whole blood; however, CCA4 were from platelet concentrates collected from apheresis. Frozen batches were received, left overnight at 4°C, and then placed in a 37°C water bath for two hours for additional thawing. The hPL was used in the same HCE-T growth medium to replace FBS. Both 5% and 10% hPL of each batch and a mixed hPL made by equal mixing of three batches were tested.

IncuCyte Zoom was used to analyze the growth of HCE-T cells. Cells were seeded in their respective media in IncuCyte ImageLock 96-well plates (Essen

Table. Nine Bioink Formulations Tested With Their Separate Component Compositions Listed

Ink	Component One	Component Two	Final Concentration
1	20% hPL 0.4mg/mL Fibrinogen DMEM/F12	2U/mL Thrombin DMEM/F12	10% hPL 0.2 mg/mL Fibrinogen 1 U/mL Thrombin
2	20% hPL 4mg/mL Fibrinogen DMEM/F12	2U/mL Thrombin DMEM/F12	10% hPL 2 mg/mL Fibrinogen 1U/mL Thrombin
3	20% hPL 10mg/mL Fibrinogen DMEM/F12	2U/mL Thrombin DMEM/F12	10% hPL 5 mg/mL Fibrinogen 1 U/mL Thrombin
4	20% hPL 0.4mg/mL Fibrinogen DMEM/F12	10U/mL Thrombin DMEM/F12	10% hPL 0.2 mg/mL Fibrinogen 5 U/mL Thrombin
5	20% hPL 4mg/mL Fibrinogen DMEM/F12	10U/mL Thrombin DMEM/F12	10% hPL 2 mg/mL Fibrinogen 5 U/mL Thrombin
6	20% hPL 10mg/mL Fibrinogen DMEM/F12	10U/mL Thrombin DMEM/F12	10% hPL 5 mg/mL Fibrinogen 5 U/mL Thrombin
7	20% hPL 0.4mg/mL Fibrinogen DMEM/F12	20U/mL Thrombin DMEM/F12	10% hPL 0.2 mg/mL Fibrinogen 10 U/mL Thrombin
8	20% hPL 4mg/mL Fibrinogen DMEM/F12	20U/mL Thrombin DMEM/F12	10% hPL 2 mg/mL Fibrinogen 10 U/mL Thrombin
9	20% hPL 10mg/mL Fibrinogen DMEM/F12	20U/mL Thrombin DMEM/F12	10% hPL 5 mg/mL Fibrinogen 10 U/mL Thrombin

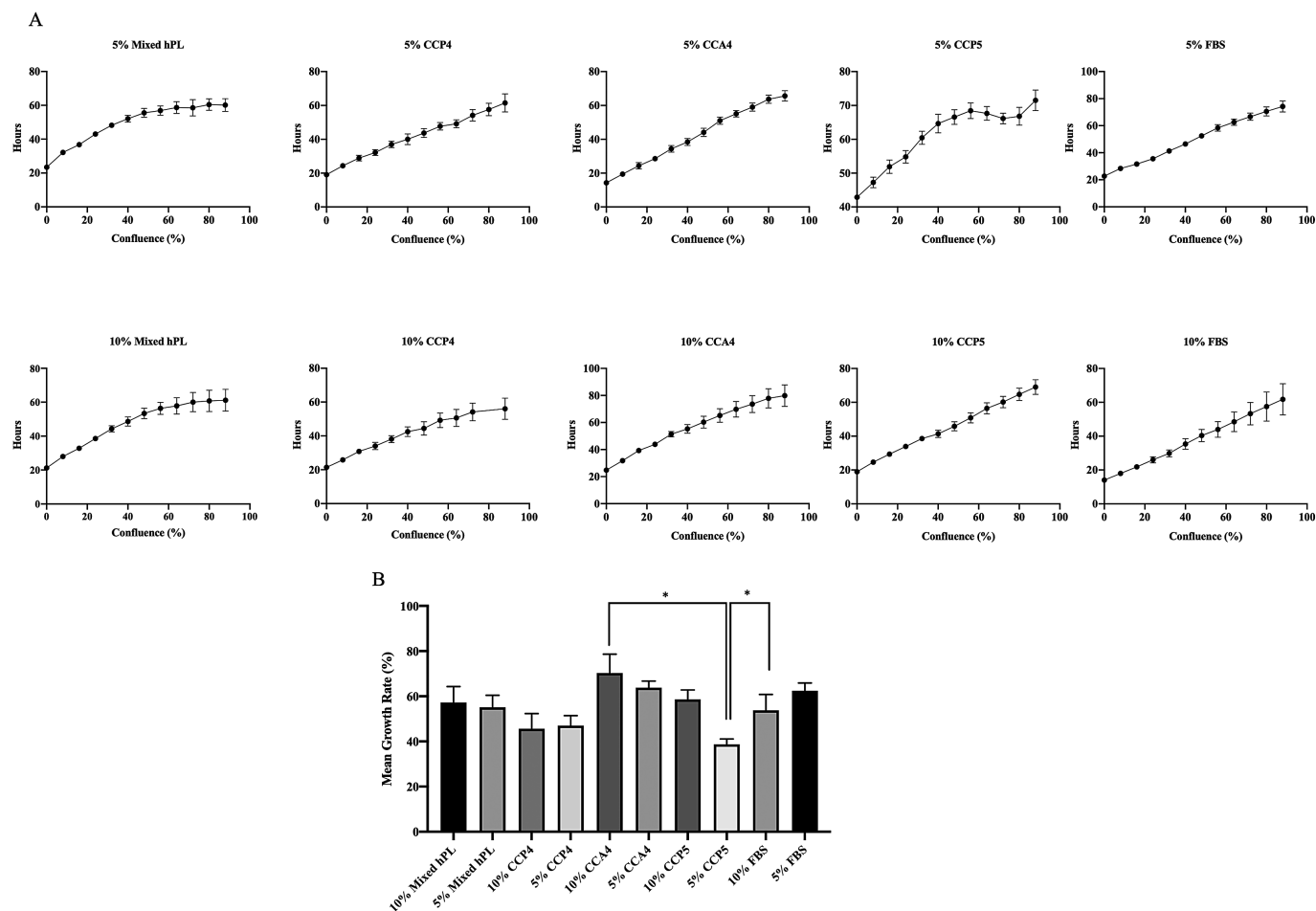


Figure 1. Comparison of effect of various hPL batch and FBS on corneal epithelial cell growth. **(A)** Confluence curve generated for each test condition showing cells can reach 100% confluence in all conditions. **(B)** Mean growth rate analysis showed that cells treated with 5% CCP5 had the lowest mean growth rate, which is significantly lower than 10% CCA4 and 10% FBS.

BioScience, Ann Arbor, MI, USA) with a negative control using Dulbecco's modified Eagle medium (DMEM)/F12 buffer. In each condition, 10,000 cells were seeded per well with respective growth medium and six technical repeats per condition conducted. These cells were left to adhere overnight. The wells were rinsed three times with PBS (pH 7.4) before changing the media the following day. The plate was placed inside the IncuCyte Zoom in a 37°C humidified incubator with 5% CO₂, and imaged every two hours for seven days. The media was changed every two days.

The percentage of confluence was calculated by the IncuCyte Zoom 2016A software (Essen BioScience) after being trained on a subset of images of HCE-T cells. The calculation was conducted for two additional repeats on the experiment (no. of wells = 18 total for each condition). The data was collated and graphed using Prism (GraphPad, San Diego, CA, USA). Mean

growth rate was calculated as $\frac{\Delta \text{confluence} (\%) }{\text{hours}}$ (change in % confluence/duration of experiment) and compared using a one-way ANOVA.

Scratch Assay to Evaluate the Effect of hPL on HCE-T Cells Wound Healing

IncuCyte Zoom analysis was used. Similar to the above experiment, cells were seeded into the IncuCyte ImageLock 96-well plate under FBS, hPL and DMEM/F12-only conditions (10,000 cells per well, $n = 6$ per condition). Batch CCP4 hPL at 5% was used to replace FBS in standard HCE-T growth medium. Cells with DMEM/F12-only condition were considered negative controls. Cells were left to grow until confluency was obtained, then the wells were scratched using the 96-WoundMaker (Essen BioScience) followed by rinsing with PBS to remove

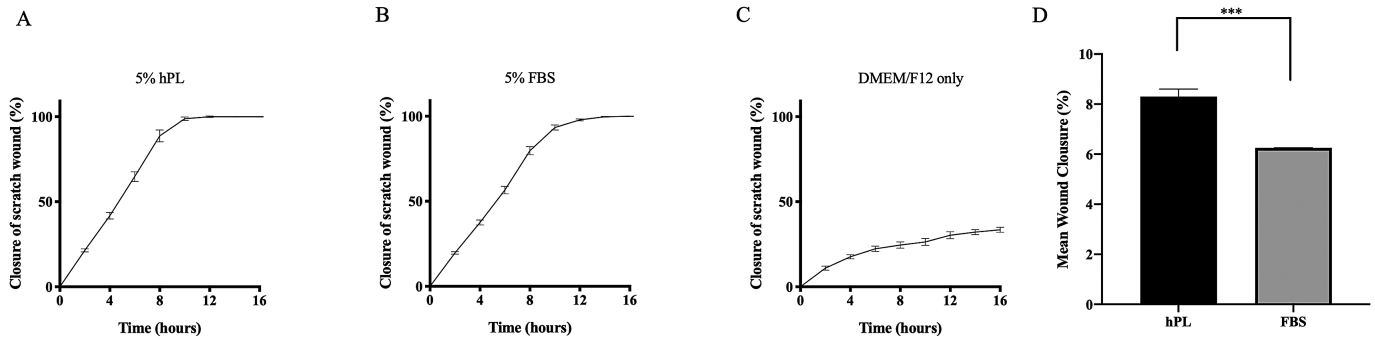


Figure 2. Significantly higher wound closure rate was found in hPL treated compared to FBS group ($P < 0.05$), and DMEM/F12 only group showed no closure of the wound as a negative control. Treatment conditions: (A) hPL, (B) FBS, and (C) DMEM only. (D) Comparison of the mean healing rate among the conditions.

the debris. The plate was placed inside the IncuCyte Zoom in a 37°C humidified incubator with 5% CO₂ and were then imaged every two hours (IncuCyte) for 16 hours. The relative wound density was calculated by the IncuCyte Zoom software after being trained on a subset of images of HCE-T cells and defined as the percentage of confluence in the wound area relative to the original wound area. This calculation was repeated for two additional repeats on the experiment (no. of wells = 18 total for each condition). The data were collated and graphed using Prism) and compared by use of a one-way ANOVA.

Various hPL Based Bioink Prepared with Transparency and a Drawing Test

Fibrinogen and thrombin were used to prepare an hPL-based bioink. The hPL-based bioink was made by equal mixing of two separate components: (i) containing hPL and fibrinogen in DMEM/F12; and (ii) containing thrombin in DMEM/F12. Fibrinogen (Merck Millipore, Kenilworth, NJ, USA) was dissolved in sterile water at 37°C and aliquoted into 1 mL Eppendorf tubes at a concentration of 20 mg/mL. These were stored at –20°C and thawed at 37°C immediately before use. Thrombin (Merck Millipore) was dissolved in DMEM/F12 and aliquoted into 1 mL Eppendorf tubes at a concentration of 20 U/mL. These were stored at –20°C and thawed at 37°C immediately before use. Various concentrations of fibrinogen (0.2, 2 and 5 mg/mL) and thrombin (1, 5, and 10 units/mL) were mixed and examined for gel formation. All bioinks contained a final concentration of 10% hPL (Table).

Total light transmittance in visible light range was measured using a ColourQuest XE (HunterLab, Reston, VA, USA) spectrophotometer. CIE L*a*b* (CIELAB) system are applied to describe the values,

where the value L (luminosity) represents the level of light or dark ranging from white (L = 100) to dark (L = 0). The machine was zeroed for a glass slide and samples of 1 mm in thickness were subsequently placed on the slide ($n = 3$ per sample) and measured. To demonstrate the potential of printability, a drawing test was conducted by writing “Cornea” with the ink on glass slide.

Rheological Examination

The rheological properties of the prepared inks were examined by an AR-G2 rheometer (TA Instruments, New Castle, DE, USA). A 2°/40 mm cone plate geometry was used in all tests. An oscillatory time sweep test was conducted to determine the consistency of the ink at 1% strain and 1 HZ frequency. The temperature was also kept constant at 34°C to mimic the temperature at the corneal surface. The effect of temperature variation on crosslinking was also investigated by varying the temperature from 10°C to 40°C.

Cell Compatibility in Bioinks

HCE-T cells were seeded in a 96 well plate (6000 cells/well) in the standard HCE-T growth medium with 10% hPL replacing FBS and were then left overnight to attach. The following morning, the wells were rinsed three times with PBS, and the media was replaced with the bioinks (Table, $n = 6$ per condition). Confluency was measured every two hours over seven days using IncuCyte ZOOM as described in the proliferation experiment. The data were tabulated, graphed, and analyzed using Prism (GraphPad).

Wound Healing Test in Ulcerated Cornea

Two ex vivo, ulcerated, human corneas that did not meet transplantation quality requirements and were rejected for transplantation were used in this test, and all studies complied with the regulations of the

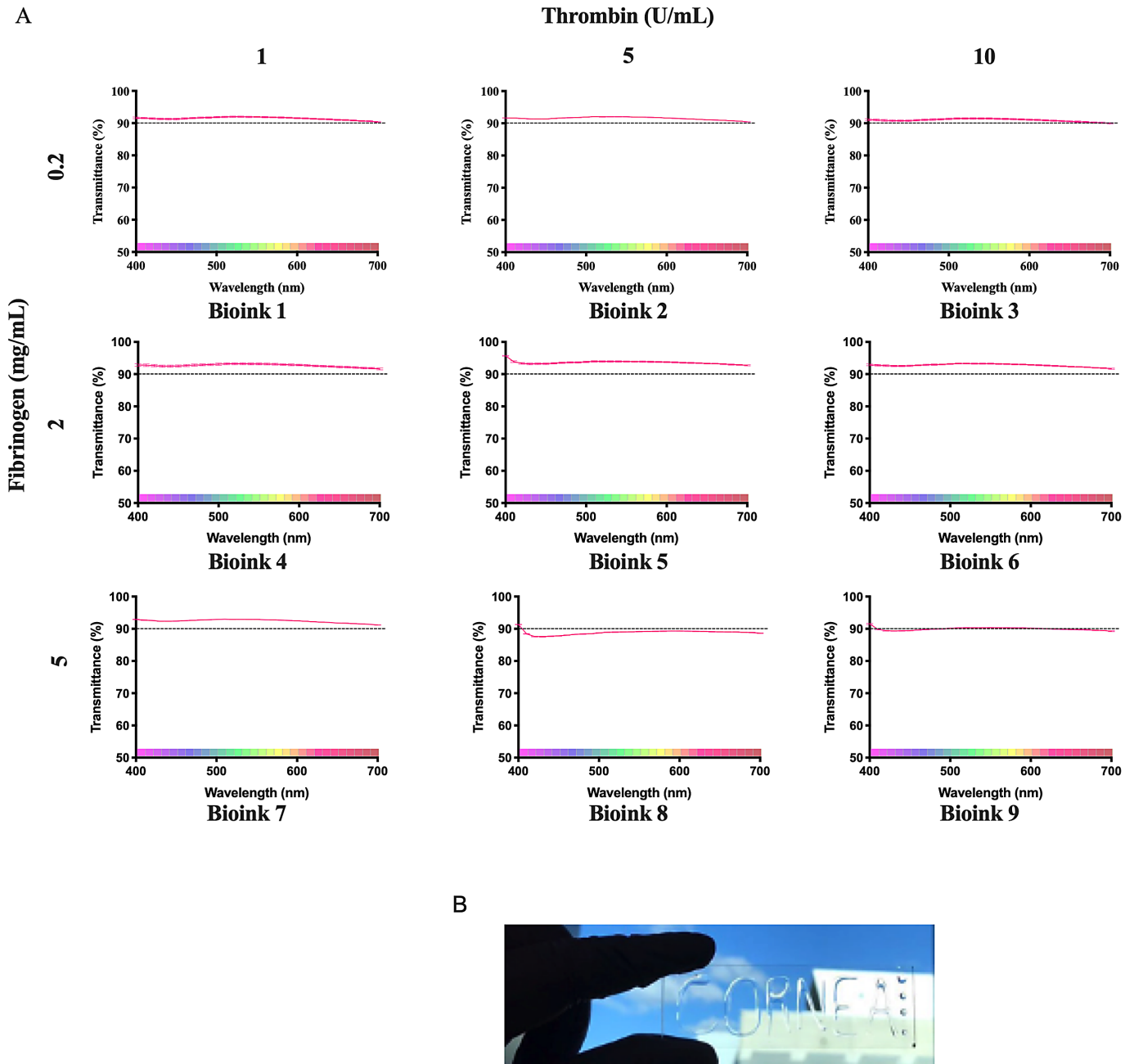


Figure 3. Bioinks tested showed high transparency. (A) Mean percentage transmittance across wavelengths of the visible spectrum (400–700 nm) ± SEM for various bioinks showed that most bioinks have great than 90% transmittance except bioinks 8 and 9. (B) A representative image of the gel formed by the formulation.

local ethics committee (HERC 14/275). The wound surface of the ulcerated cornea that had been removed postmortem was debrided with a surgical spade, and then the bioink 5 was administered over the wound surface. The cornea was then suspended in a jar of organ culture media via a thread connecting the cornea to the lid of jar, which represented standard storage Eye Bank protocol. The ink was reapplied at days

1 and 4. All handling was conducted using aseptic techniques in a tissue culture hood. The cornea was fixed in 4% paraformaldehyde (PFA) at day 7 and then cryosectioned (12 μm) and stained with H&E. The second cornea served as a control and had no bioink applied to the surface wound. The specimen was suspended in a jar the same way as the treated cornea.

Results

The Effect of hPL Source on HCE-T cell Growth

HCE-T cells cultured on tissue culture plates in the FBS and hPL media all reached full confluence at approximately 2 days in IncuCyte Zoom (Fig. 1A). The highest mean growth rate observed was at 70.3% ± 8.3% (±SEM) for cells treated with 10% CCA4 hPL batch, and the lowest rate detected at 38.7% ± 2.4 in cells treated with 5% CCP5 (Fig. 1B). Comparison between different hPL batches, mixed hPL and FBS at the same concentration (5% and 10%) showed no significant difference. Comparing between 10% and 5% hPL, FBS and mixed hPL showed that 10% CCA4 and 10% FBS had significant higher effect than 5% CCP5 treatment on cell growth rate ($P < 0.05$, Fig. 1B), but

no significant difference was observed in the rest of the samples.

The Effect of hPL on HCE-T Wound Healing

Cells in the FBS and hPL (CCP4) conditions all obtained full scratch wound closure after approximately 12 hours, and with the negative control (DEME/F12) scratch wound closure was not achieved after 16 hours (Figs. 2A–2C). The mean wound closure rate was significantly higher in the presence of 5% hPL at 8.33% ± 0.29% (±SEM) compared to 5% using FBS media at 6.25% ± 0.01% (±SEM) ($P < 0.0001$, Fig. 2D).

Bioink Formulation

Visual observations confirmed that all components (i and ii) in labeled bioink samples 1 to 9 (Table) were

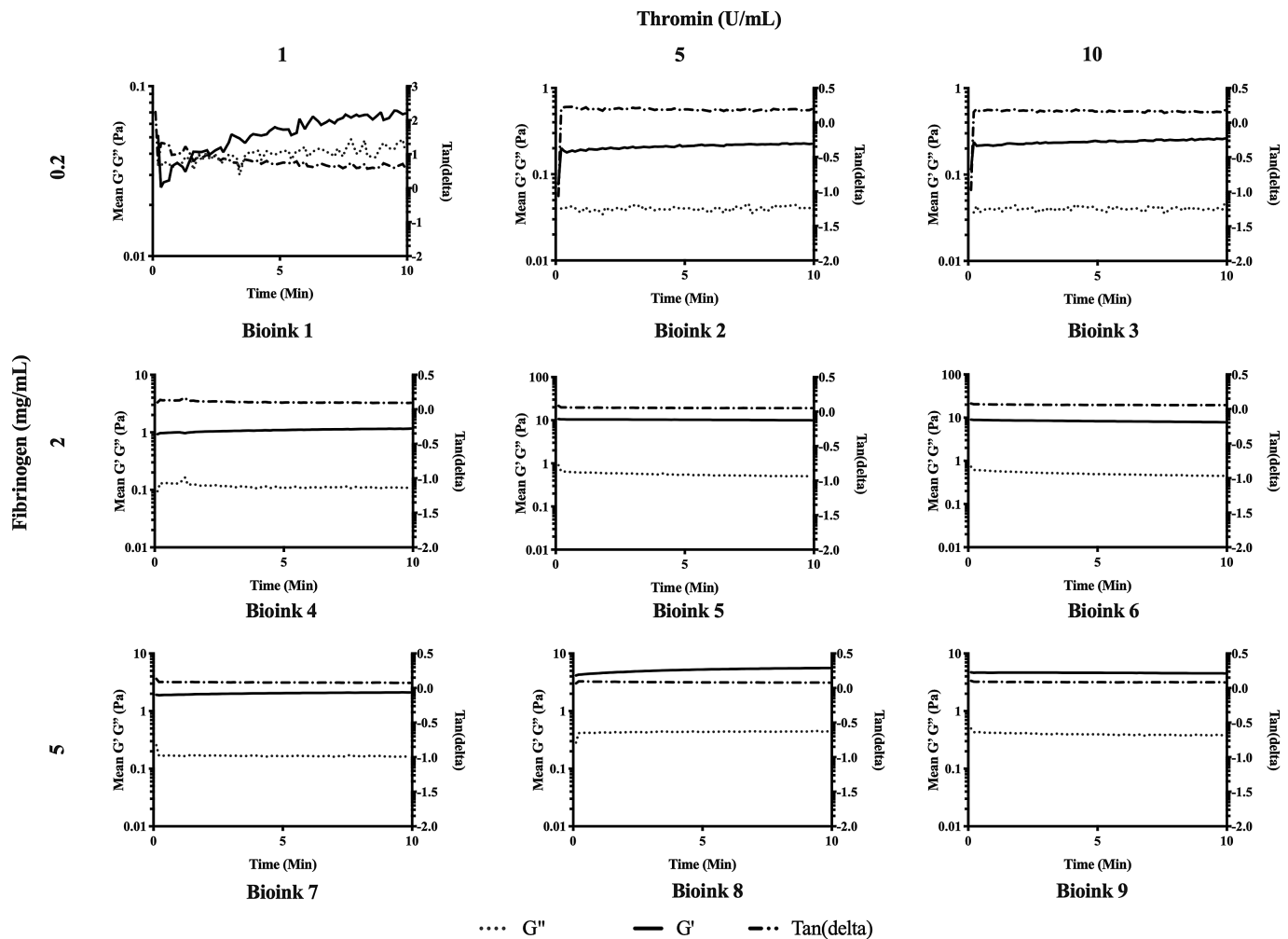


Figure 4. Storage (G'), loss (G'') moduli and $\tan(\delta)$ of the various bioinks ± SEM over a time-sweep oscillation of 1Hz at 34°C for 10 minutes for each bioink.

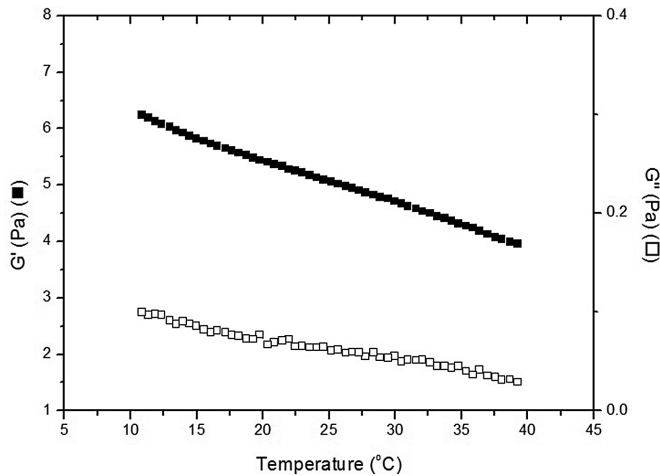


Figure 5. Storage (G') of bioink 5 is higher than loss (G'') moduli across 10°C to 40°C.

liquids that formed a clear gel when mixed. All bioinks (except bioinks 8 and 9) achieved more than 90% total light transmittance (bioink 8 had transparency just below 90%, and bioink 9 is at 90%) (Fig. 3A). The drawing test showed that the bioink reattains a structural form and adhered to the glass substrate enabling the word “Cornea” to be printed (Fig. 3B).

Rheologic Properties

The rheology result showed that with the exception of bioink 1, the storage modulus (G') exceeded the loss modulus (G'') across all time points in all other bioink formulations. However, bioink 5 had the highest G' at around 10 Pa (Fig. 5). The variation of modulus values and $\tan \delta$ was negligible over the 10-minute test period. Although Bioink 5 showed a stable modulus at 34°C, a decrease was observed on both G' and G'' when the temperature was varied from 10°C to 40°C.

Cell Compatibility of Vairous Bioink

Incucyte Zoom results demonstrated that the HCE-T were able to reach full confluency in seven days on all bioinks except bioinks 6 and 9 (Fig. 6). The growth rate did not increase in bioinks 6 and 9 and was significantly lower than bioinks 7 and 8 (Fig. 6).

Ex Vivo Cornea Wound Healing

Bioink 5 was used in the ex vivo study. The H&E section results showed complete re-epithelization in the bioink 5-treated cornea, whereas no re-epithelization was observed in the control cornea (Fig. 7). Multiple layers of the bioink could be observed in the recovered epithelium.

Discussion

We have developed a transparent two-part bioink consisting of part 1 containing hPL, fibrinogen, and DMEM/F12, and part 2 with thrombin in DMEM/F12 that when printed provides the key properties required for extrusion-based printing. In this study, we first examined the effect of hPL on corneal epithelial cell growth and wound healing. Three different batches of hPL (CCA4, CCP4, and CCP5) with concentration of 10% (v/v) and 5% were compared, noting only 10% CCA4 was found to exhibit a significantly higher cell growth than 5% CCP5. No difference was found among the hPL used at the same concentration. CCA4 platelets that came from apheresis process had more plasma content than platelets collected from whole blood (CCP4 and CCP5), and this may contribute to the significant difference between 10% CCA4 and 5% CCP5. However, differences did appear to be ameliorated by increasing the concentration of hPL, because no significant difference was observed between 10% CCA4 and 10% CCP5. This is possibly due to the saturation of growth factors. To minimize irregularity caused by batch-batch variation in the scratch wound assay, we used 5% CCP4 and showed that hPL significantly increased the rate of wound closure compared to FBS. Our results are consistent with previous published results^{27,28} showing hPL has a positive effect on epithelial cell proliferation and wound healing. These findings also suggest that standard preparation protocols and strict quality control is essential when using hPL in cell culture. Nevertheless, we believe it is reasonable to hypothesize that a bioink containing hPL will facilitate wound healing.

In addition to hPL, fibrinogen and thrombin were included to facilitate the cross-linking process. The bioink components comprised two parts: fibrinogen and hPL as one part, and thrombin as the other. All the reagents were dissolved in DMEM/F12, providing a suitable buffer for the bioink cell compatibility tests. No cross-linking was observed when hPL was mixed with fibrinogen in DMEM/F12 buffer. In all the formulations tested, all of them formed a gel after mixing. We also conducted a drawing test by writing “cornea” in a glass slide using the ink, and the success of this test showed it behaved as an “ink.”

Rheology tests were conducted to show the rheological properties of the ink, which enabled prediction of their behavior during and after 3D printing. The comparison of the storage modulus (G'), loss modulus (G''), and $\tan \delta$ of nine formulations versus time showed that samples 2 to 9 had G' larger than G'' approximately by a factor of

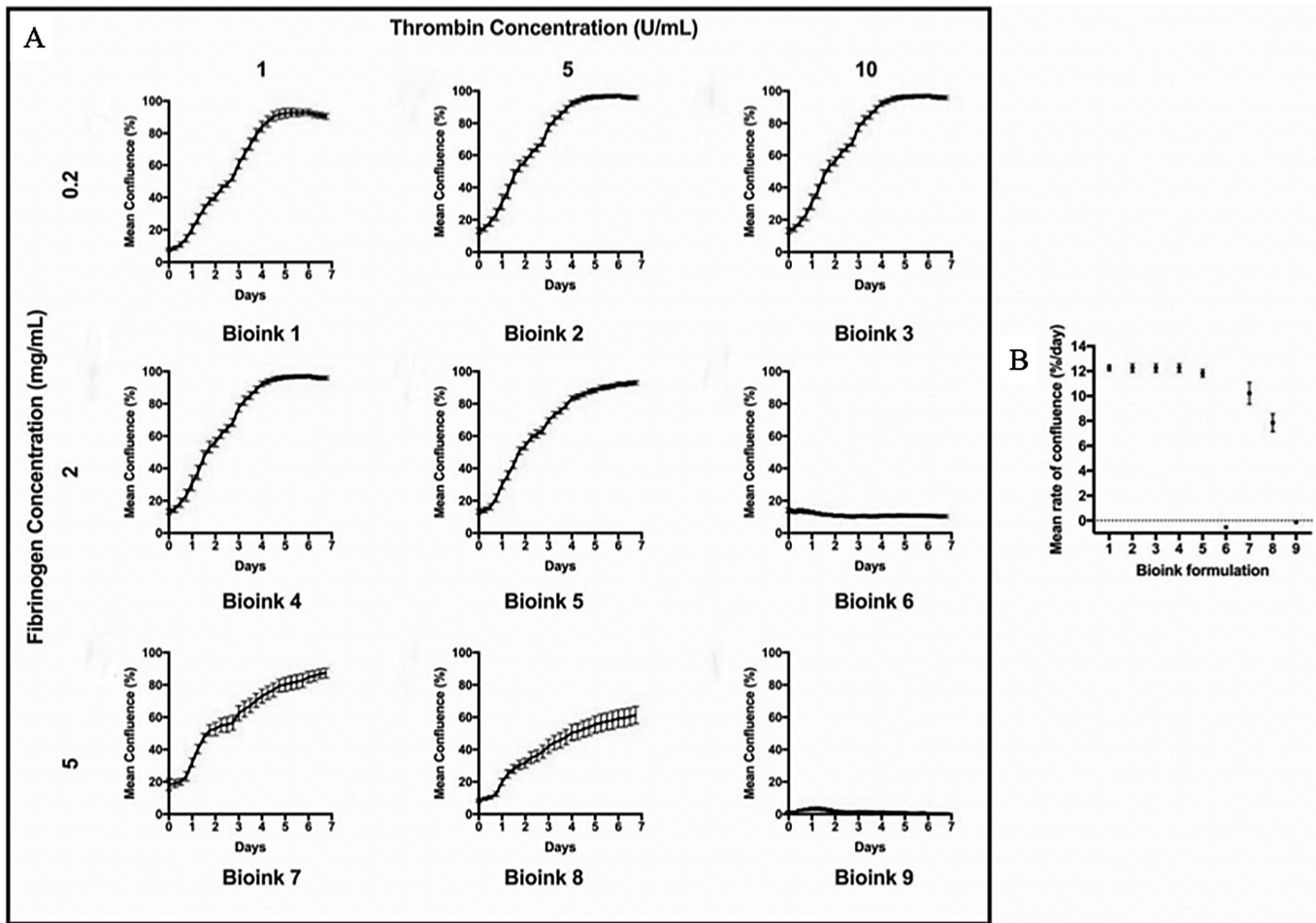


Figure 6. Corneal epithelial cell confluence can be reached in majority of bioinks within 1 week (except bioinks 6, 8, and 9). (A) percentage of confluence for corneal epithelial cells cultured at a density of 6,000 cells per bioink ($n = 6$ per condition). (B) The mean rate of confluence as a percentage per day for all nine bioinks.

10 regardless of the formulation (Fig. 4). This result indicated that the ink demonstrates elastic behavior in its linear viscoelastic range capable of maintaining its shape after cross-linking. There was a minimum variation in modulus values of the samples and $\tan \delta$ (G''/G') remained almost constant in 10 minutes, indicating stable viscoelastic behavior of the ink in this time frame at 1% strain. Increased fibrinogen and thrombin did not correlate to increased modulus values, instead the results showed the middle ranges of bioinks, bioink 5 with final mixed fibrinogen at 2 mg/mL and thrombin concentration at 5 U/mL, had the highest storage modules at 10 minutes. Bioink 1 showed a different behavior from the other formulations evident by the relatively low modulus with an unstable increasing trend. This indicates that, in contrast to the other samples, bioink 1 did not undergo effective cross-linking. This may be attributed to the low fibrinogen and thrombin concentrations used.

The rheological properties of Bioink 5 was further investigated as it showed a high potential to be selected as the optimum formulation due to its better stiffness and cell compatibility. The effect of temperature (from 10°C to 40°C) on the modulus of bioink 5 showed that G' remained greater than G'' over the temperature range. It also showed decreasing G' with increasing temperature, denoting a reduction in elastic properties of the sample. With G' at about 4.5Pa at 34°C, this bioink would remain stable on the surface of cornea due to G' greater than G'' , but it would unlikely be used as a sole material to substitute corneal stroma.

The light transmittance tests showed that all the inks have greater than 80% light transmittance, with bioinks 1 to 7 having transmittance over 90%, whereas bioinks 8 and 9 have transmittance just below and equal to 90%. This result suggests that higher fibrinogen and thrombin concentration may impact the light transmittance.

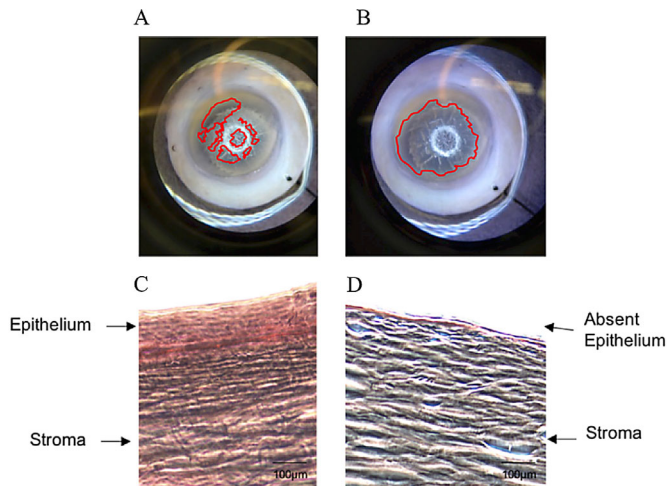


Figure 7. Re-epithelialization of an ex vivo, ulcerated, human cornea that had been previously rejected for transplant use. iFixInk was applied at days 1 and 4 and fixed, cryosectioned, and stained with H&E at day 7. (A) The initial ulcer, with the ulcerated regions emphasized in red. (B) The size of the epithelial-free surface after wound-debriding. (C) H&E staining of the central part of the cornea shows complete re-epithelialization with a thickness and morphology comparable to that of a healthy human cornea. (D) H&E staining of the central part of a de-epithelialized cornea for comparison.

Cytocompatibility tests on all bioinks revealed that the use of higher fibrinogen and thrombin reduced cell growth (Fig. 6). Cells were unable to reach confluence within seven days for bioinks 6 to 9 (final fibrinogen concentration ≥ 5 mg/mL and thrombin > 10 U/mL). Combined, these findings suggest that within the tested range, fibrinogen and thrombin concentrations were associated with a decreased storage module and light transmittance, with the former in a bell curve manner and the latter likely in an increasing linear trend. We suggest that 5 mg/mL of fibrinogen combined with 10 U/mL thrombin is likely to represent the threshold effect on corneal epithelial cell growth.

Key criteria required for the successful extrusion of printed bioink for corneal-related applications include the ability to undergo a phase transition to maintain the shape, transparency and cytocompatibility. The optimal formulation for the bioink was chosen by combining the best cell compatibility and mechanical properties. The transmittance of human cornea has a reported number at around 90% in visible light range²⁹ and therefore is a benchmark for transparency selection. Cell compatibility is a critical element, and the selected bioink should be at the higher end in its effect on cell confluence. Bioink 5, with a final composition consisting of 10% hPL, 2 mg/mL fibrinogen, and 5 U/mL thrombin, met all the selection criteria and therefore was selected for the ex vivo corneal wound healing test.

The ex vivo corneal wound healing test was designed to examine the hypothesis that the bioink can facilitate the wound healing. The result unequivocally indicated that an ulcerated cornea treated with the bioink was able to regenerate a full-thickness corneal epithelium. Although the test procedure demonstrated wound healing potential and the adhesive properties of the bioink to the surface of cornea, this remains a single example. The logical progression will be to conduct animal trials to evaluate the effect of this bioink in-vivo.

The composition of this newly developed potential bioink is closest to the bioink developed by Sorkio et al.²¹ in that all proteins were of human origin, and we also used a blood-derived product hPL. The ingredients used in our bioinks have already been used in human clinical applications. Fibrinogen and thrombin have been widely used as a tissue glue in clinics including ophthalmic surgeries³⁰ and hPL has also been used in corneal surgeries.¹⁸ Our developed bioink should therefore be safe to be used in human. In comparison to the commercially available fibrin glue that is not transparent and uses high concentrations of fibrinogen (70–80 mg/mL) and thrombin (500–1000 U/mL),³¹ our hPL-based product contained much less fibrinogen (2 mg/mL) and thrombin (5 U/mL) and is transparent with a total light transmittance over 90% and therefore suitable to be applied on clear tissues such as the cornea.

In addition to the composition differences to these prior developed bioinks and the fibrin glue, our developed bioink has the potential to facilitate re-epithelialization likely as a result of the inclusion of hPL. Our results showed that the bioink can regenerate multilayered corneal epithelium in ex vivo human corneas. Although a single sample, this demonstrated its potential in treating corneal wounds. In vivo tests are required to confirm our current findings. It is unclear at this stage whether our bioink is capable of being used to bioengineer a functional bioengineered cornea, primarily because we cannot demonstrate whether the bioink can be used to print a multilayer corneal structure. A customized printer is required to demonstrate this ability. However, our bioink is easy to prepare and can be applied to the cornea with adequate adhesion. In summary, we have developed a unique transparent bioink incorporating hPL. Our findings showed that this bioink can be printed in situ directly onto the wounded cornea to allow re-epithelialization of the ulcerated cornea and facilitate earlier recovery. The bioink represents a novel approach to treat injured corneas, potentially avoiding long-term visually limiting sequelae. This may lead to significant benefits, particularly in developing countries where access to

specialist services and corneal tissue is severely limited. Further animal tests are required for validation.

Acknowledgments

The authors thank Donna Lai and Sheng Hua from the Molecular Biology Facility, Bosch Institute, University of Sydney for providing training and equipment required for tissue culturing, Incucyte zoom testing and analysis; and Australian Red Cross to provide hPL samples. We also acknowledge the Australian National Fabrication Facility (ANFF) Materials Node for their provision of equipment and materials, and facilities support within the University of Wollongong Electron Microscopy Centre.

Supported by the Australian Research Council (ARC) Centre of Excellence Scheme (CE140100012), Sydney Eye Hospital Foundation and Lions NSW Eye Bank.

Disclosure: **H. Frazer** (P); **J. You**, iFix Medical (P, I, F); **Z. Chen**, None; **S. Sayyar**, None; **X. Liu**, None; **A. Taylor**, None; **C. Hodge**, None; **G. Wallace**, None; **G. Sutton**, iFix Medical (P, I)

References

1. Flaxman SR, Bourne RRA, Resnikoff S, et al. Global causes of blindness and distance vision impairment 1990–2020: a systematic review and meta-analysis. *Lancet Glob Health*. 2017;5:e1221–e1234.
2. Oliva MS, Schottman T, Gulati M. Turning the tide of corneal blindness. *Indian J Ophthalmol*. 2012;60:423–427.
3. Whitcher JP, Srinivasan M, Upadhyay MP. Corneal blindness: a global perspective. *Bull World Health Organ*. 2001;79:214–221.
4. McCarty CA, Fu CL, Taylor HR. Epidemiology of ocular trauma in Australia. *Ophthalmology*. 1999;106:1847–1852.
5. Ashby BD, Garrett Q, Willcox MD. Corneal injuries and wound healing—review of processes and therapies. *Austin J Clin Ophthalmol*. 2014;1:1–25.
6. Saghizadeh M, Kramerov AA, Svendsen CN, Ljubimov AV. Concise review: stem cells for corneal wound healing. *Stem Cells*. 2017;35:2105–2114.
7. Hossain P. The corneal melting point. *Eye (Lond)*. 2012;26:1029–1030.
8. Voiculescu OB, Voinea LM, Alexandrescu C. Corneal neovascularization and biological therapy. *J Med Life*. 2015;8:444–448.
9. Mathews PM, Lindsley K, Aldave AJ, Akpek EK. Etiology of global corneal blindness and current practices of corneal transplantation: a focused review. *Cornea*. 2018;37:1198–1203.
10. Giannaccare G, Versura P, Buzzi M, Primavera L, Pellegrini M, Campos EC. Blood derived eye drops for the treatment of cornea and ocular surface diseases. *Transfus Apher Sci*. 2017;56:595–604.
11. Tsubota K, Goto E, Shimmura S, Shimazaki J. Treatment of persistent corneal epithelial defect by autologous serum application. *Ophthalmology*. 1999;106:1984–1989.
12. Suri K, Gong HK, Yuan C, Kaufman SC. Human platelet lysate as a replacement for fetal bovine serum in limbal stem cell therapy. *Curr Eye Res*. 2016;41:1266–1273.
13. Murphy SC, Vassallo R, Murphy S. Preservation and clinical use of platelets. In: *Williams Hematology*. 6th ed. New York: McGraw-Hill Medical; 2001:1905–1916.
14. van der Meer PF, Seghatchian J, Marks DC. Quality standards, safety and efficacy of blood-derived serum eye drops: a review. *Transfus Apher Sci*. 2016;54:164–167.
15. De Pascale MR, Sommese L, Casamassimi A, Napoli C. Platelet derivatives in regenerative medicine: an update. *Transfus Med Rev*. 2015;29:52–61.
16. Crovetti G, Martinelli G, Issi M, et al. Platelet gel for healing cutaneous chronic wounds. *Transfus Apher Sci*. 2004;30:145–151.
17. Alio JL, Rodriguez AE, Martinez LM, Rio AL. Autologous fibrin membrane combined with solid platelet-rich plasma in the management of perforated corneal ulcers: a pilot study. *JAMA Ophthalmol*. 2013;131:745–751.
18. Alio JL, Rodriguez AE, Martinez LM. Bovine pericardium membrane (tutopatch) combined with solid platelet-rich plasma for the management of perforated corneal ulcers. *Cornea*. 2013;32:619–624.
19. Anitua E, Sanchez M, Nurden AT, et al. Autologous fibrin matrices: a potential source of biological mediators that modulate tendon cell activities. *J Biomed Mater Res A*. 2006;77:285–293.
20. Isaacson A, Swioklo S, Connon CJ. 3D bioprinting of a corneal stroma equivalent. *Exp Eye Res*. 2018;173:188–193.
21. Sorkio A, Koch L, Koivusalo L, et al. Human stem cell based corneal tissue mimicking structures

- using laser-assisted 3D bioprinting and functional bioinks. *Biomaterials*. 2018;171:57–71.
22. Ferris CJ, Gilmore KG, Wallace GG, In het Panhuis M. Biofabrication: an overview of the approaches used for printing of living cells. *Appl Microbiol Biotechnol*. 2013;97:4243–4258.
 23. Di Bella C, Duchi S, O’Connell CD, et al. In situ handheld three-dimensional bioprinting for cartilage regeneration. *J Tissue Eng Regen Med*. 2018;12:611–621.
 24. Kilic Bektas C, Hasirci V. Cell loaded 3D bioprinted GelMA hydrogels for corneal stroma engineering. *Biomater Sci*. 2019;8:438–449.
 25. Kim H, Park MN, Kim J, Jang J, Kim HK, Cho DW. Characterization of cornea-specific bioink: high transparency, improved in vivo safety. *J Tissue Eng*. 2019;10:2041731418823382.
 26. Chung JHY, Naficy S, Yue Z, et al. Bio-ink properties and printability for extrusion printing living cells. *J Biomater Sci*. 2013;1:763–773.
 27. Zhang J, Crimmins D, Faed JM, Flanagan P, McGhee CNJ, Patel DV. Characteristics of platelet lysate compared to autologous and allogeneic serum eye drops. *Transl Vis Sci Technol*. 2020;9:24.
 28. Chen LW, Huang CJ, Tu WH, et al. The corneal epitheliotropic abilities of lyophilized powder form human platelet lysates. *PLoS One*. 2018;13:e0194345.
 29. Meek KM, Knupp C. Corneal structure and transparency. *Prog Retin Eye Res*. 2015;49:1–16.
 30. Kumar N, Al Sabti K. Fibrin glue in ophthalmology. *Indian J Ophthalmol*. 2010;58:176.
 31. Spotnitz WD. Fibrin sealant: the only approved hemostat, sealant, and adhesive—a laboratory and clinical perspective. *ISRN Surg*. 2014;2014:203943.